About the physical meaning of the critical temperature for catastrophic optical damage in high power quantum well laser diodes

J Souto, J L Pura, and J Jiménez

GdS Optronlab, Departamento de Física de la Materia Condensada, Ed. I+D, Universidad de Valladolid, P. de Belén 11, 47011 Valladolid, Spain

E-mail: souto@eii.uva.es

Short title: About the physical meaning of the critical temperature for catastrophic optical damage

Classification numbers: 02.70.Dh; 42.55.Px; 65.40.De; 68.60.-p

Keywords: catastrophic optical damage, critical temperature, thermal conductivity, high power laser diode, finite element methods

About the physical meaning of the critical temperature for catastrophic optical damage

Abstract

It is usually assumed that the catastrophic optical damage of high power laser diodes is launched when a critical local temperature (Tc) is reached; temperatures ranging from 120ºC to 200ºC were experimentally reported. However, the physical meaning of Tc in the degradation process is still unclear. In this work we show that, in the presence of a local heat source in the active region, the temperature of the laser structure, calculated using finite element methods, is very inhomogeneously distributed among the different layers forming the device. This is due to the impact that the low dimensionality and the thermal boundary resistances have on the thermal transport across the laser structure. When these key factors are explicitly considered, the quantum well (QW) temperature can be several hundred degrees higher than the temperature of the guides and cladding layers. Due to the size of the experimental probes, the measured critical temperature is a weighted average over the QW, guides and claddings. We show the existence of a great difference between the calculated average temperature, equivalent to the experimentally measured temperature, and the peak temperature localized in the QW. A parallel study on double heterostructure lasers is also included for comparison.

1. Introduction

The catastrophic optical damage (COD) of high power laser diodes (LD) is a harmful degradation mode. In this failure mode the optical output power undergoes a sudden drop after many hours of normal operation. The COD is usually described as a thermal runaway process, in which the temperature is locally enhanced; this temperature increase shrinks the band gap of the active zone, with the corresponding enhancement of the optical absorption, ending by the melting of the active zone in a feedback process. Local temperature increase plays a paramount role in the occurrence of the laser degradation; therefore, the temperature measurement of the active zone of the laser during operation is a critical issue to assess the degradation mechanism. The occurrence of a local critical temperature (Tc, which, once reached, launches the COD process, has been reported by different authors [1-4] and has been tentatively explained in terms of various physical-mathematical models [5-8]. Experimental measurements in lasers under operation give Tc values ranging from 120ºC to 200ºC depending on the lasers [1]. Usually, this temperature is measured at the laser front facet; albeit, it has also been measured inside the cavity for lasers showing internal COD [2]. These critical temperatures are surprisingly low, and the understanding about their physical meaning is ambiguous. Furthermore, Tc is considered to be the best parameter to quantify the device resistance to damage [1]. One can summarize that a high Tc is the signature of robust devices, while low Tc is the signature of weak LDs; but, far away from this observation, one cannot argue about the physical mechanism driving the degradation of the laser structure in terms of a physical process, triggered at a so low temperature, enabling the generation of the extended defects responsible of the catastrophic device failure.

The local temperature has been routinely characterized by measuring temperature profiles of the operating devices using a variety of techniques, such as Raman microscopy (μR) [1, 2, 4], thermal infrared imaging (TII) [2], thermoreflectance (TR) [1-4], and micro-Photoluminiscence (μPL). The outcome of all these studies is limited by the size of the sampled area, with a lateral resolution slightly submicrometric for the techniques using a focused laser beam, i.e. μR, TR and μPL, and ≈3 μm at the best for TII. Therefore, the measured temperature is indeed averaged over a region two orders of magnitude larger than the QW thickness in a QW LD. This is very relevant, because the thermal transport across the multilayer structure of the laser renders the temperature distribution around the active region very inhomogeneous.

We present herein a detailed study about the temperature distribution in the active zone of the laser based in the solution of the heat transport equation when a local heat source occurs in the active zone of the laser during operation. We present a comparative analysis between QW and double heterostructure (DH) lasers, showing the relevance of the low dimensionality of the QW in the temperature distribution across the laser structure.

2. Structure of the devices

We have conducted our analysis on two types of devices for comparison purposes; namely, a graded-index separate confinement heterostructure (GRINSCH) QW laser based on an AlGaAs/GaAs broad emitter laser bar (808 nm wavelength) with optical output powers up to a few tens of watts [9], and a

DH laser, whose the active structure consists of a 200 nm thick GaAs layer confined by two $Al_{0.30}Ga_{0.70}As$ 1 μm thick cladding layers. The core of the QW device, which has been described in detail elsewhere [7], consists of a 12 nm thick $Al_{0.10}Ga_{0.90}As$ QW sandwiched in between two 130 nm thick graded barrier layers with aluminum concentrations growing from 0.26 to 0.65, and two cladding layers with 0.65 Al concentration. The substrate, as well as the soldering and heat sink, were chosen identical for both devices. The main parameters used for the calculations were taken from the sources cited in [7].

3. Computational model

The importance of the local QW temperature for the degradation process was highlighted in former works, in which we developed a thermo-mechanical model accounting for the degradation threshold of LDs [7, 9, 10]. In this model, the degradation is originated by a very local heat source in the active layer of the laser, either the QW in QW lasers, or the GaAs layer in DH lasers. This heat source, generated by the accumulation of energy in a defect rich region of the active zone, has been assumed to be uniform for the QW, whereas a Gaussian power distribution has been adopted for the GaAs layer of the DH laser. We are not focusing on the precise physical origin of the initial local heating; it is out of the present scope, though it is a very relevant point to consider in forthcoming works. Here we are dealing with the temperature distribution in the laser structure in the presence of the local heat source. Note that once the heating has started the accumulated heat is mainly due to the laser self-absorption, because of the local bandgap shrinkage. In this work, we solve by finite element methods (FEM) the heat transport equation, aiming to reproduce the temperature distribution in the laser structure induced by the local heat source. Thereafter, one proceeds to evaluate the thermal stresses generated from the inhomogeneous temperature distribution in a structure formed by layers with different properties, both thermal and mechanical. The computations have been performed within the framework of the commercially available program COMSOL Multiphysics®.

Even though the relevant role of the thermal resistivity of the active layer on the degradation of the LDs has been pointed out by some authors [11], and in spite of the experimental evidence [12-

18] regarding the influence of the layer thickness, the dislocation density and the interface roughness on the thermal conductivity of multilayer structures, all the previous computational studies about the temperature estimation during the operation of the QW LDs have systematically used bulk thermal conductivity figures. We present herein how those contributing factors [19-21] affect the temperature profile across the laser structure, resulting in a highly inhomogeneous temperature distribution around the active zone during the laser operation. Following the expression derived by Liang and Li [19] for the dependence of the thermal conductivity on the thickness of the layers and the roughness of the interfaces, we will show that the Tc usually reported for COD does not meet the true temperature reached in the QW, while it gives a more approximate value to the local temperature in DH lasers.

4. Results and discussion

An important outcome revealed by the solution of the heat transport is the large inhomogeneity of the temperature distribution around the active zone of the device. The computed temperature profiles across the QW laser structure for a local heat source (6 MW/cm^2, which is a realistic value of the laser power density absorbed) and different interface thermal resistances, are shown in Figure 1(a). The interface roughness ranges from typical values for as-prepared state-of-the-art diode lasers (2.5-5 Å, that correspond to one or two monolayers of GaAs), to larger numbers for progressively degraded devices. The results assuming a thermal conductivity identical to the bulk value have also been included in this graph. The QW temperature is notably higher than the temperature of the surrounding layers (guides and claddings). This abrupt temperature inhomogeneity is the consequence of the thermal conductivity mismatch between the AlGaAs layers with various Al contents and the QW, because of the thermal conductivity suppression associated with the low dimensionality of the QW, and the thermal barrier at the interfaces [19, 22]. The peak temperature is reached in the region of the QW, where the laser light is absorbed; we modelled here this absorption at the front facet, though it can be easily extended to the inner cavity. The temperature drastically decreases in the adjacent layers, guides and claddings. The additional suppression of the thermal conductivity resulting from increasing the interface roughness dramatically enhances this effect, resulting in higher temperatures

About the physical meaning of the critical temperature for catastrophic optical damage in the QW.

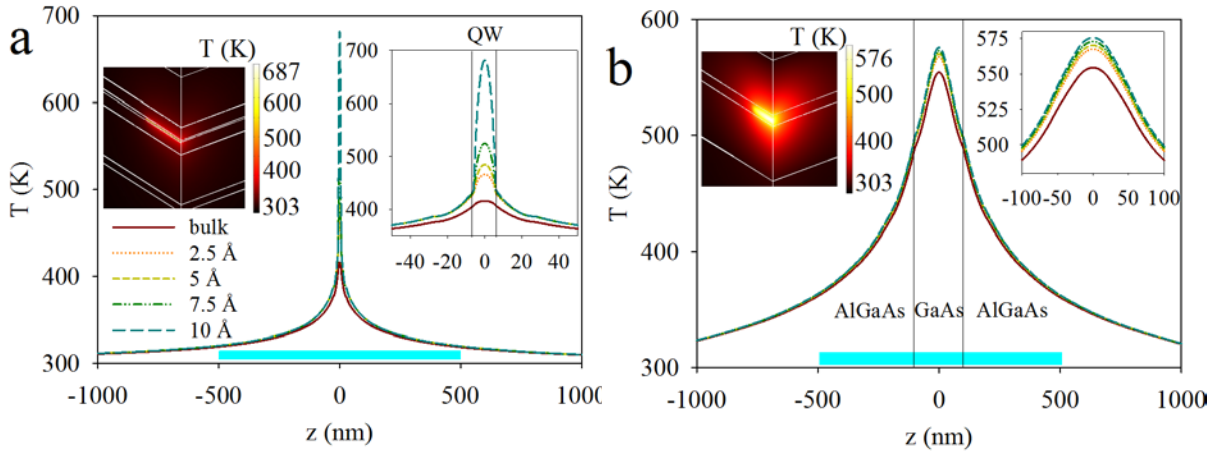

Figure 1. Temperature profiles across the growth (z) direction for the studied devices: (a) GRINSCH-QW laser under a 6 MW/cm^2 local heat source, the profiles are calculated for bulk thermal conductivity and for interface roughness ranging from 2.5 to 10 Å. A more detailed view of the active layers illustrates the progressive steepness of the temperature gradient in the QW (right insert), whereas a 3D plot with a temperature color code highlights the dramatic limitation of the heat dissipation from the QW for the 10 Å roughness case (left insert); (b) DH laser under a local Gaussian distributed heat source, with a 4 MW/cm^2 peak value, any other conditions as in (a). The profiles within the GaAs active layer are shown in the right insert, and the larger extent of the heating for the 10 Å interface roughness is depicted in the left insert. The origin of the z axis is set at the center of the QW/GaAs layers. The stripe on the x-axis under the T profiles sets the estimated size of the experimental probes (about 1 μm). The range in the vertical (z) direction for both left insert images, for which only half of the structure is depicted (the plane on the right is a symmetry plane), is approximately 1.2 μm.

For sake of comparison, we did similar calculations for the DH laser; although the temperature profiles calculated for the DH laser also show higher temperatures in the GaAs active layer, the temperature gradients are far smoother than those observed for QW lasers, Figure 1(b). This can be straightforwardly explained, as the dimensions of the active layers are about one order of magnitude larger than those of the GRINSCH-QW, and the size corrections to the thermal conductivity are considerably lower in the case of the DH laser.

As previously mentioned, the experimentally measured temperature should be the mean value averaged over the different layers simultaneously sampled by the probe beam. In order to confront the calculated data with the usually reported experimental results, we proceed to average the computed temperature distributions over the probe size of the experimental techniques (1μm x 1μm for μR, TR, or μPL). The computed peak temperatures (QW temperature) and the estimated average temperatures over the probe size are plotted in Figure 2. For the GRINSCH laser, the QW represents a very low contribution to the mean value as its lateral dimension (12 nm) is so much smaller than that of the sampled area; it can be observed that the experimentally measured Tc (corresponding in our calculation to the average temperature over the probe size, Figure 2.b) is severely underestimating the peak temperature reached in the QW (Figure 2.a). The QW temperature depends supralinearly on the optical power density, whereas the average temperature shows an almost linear relationship with that parameter. Moreover, for a given power density, the differences between the peak and the average temperatures are increasingly significant for larger interface roughnesses. The discrepancy between experimentally measured and calculated peak temperatures is also observed for the DH lasers, but the difference is far less significant than for the QW lasers. In the DH laser, the size of the active layer (200 nm) is less than one order of magnitude smaller than the probes, so that its weight on the average value is much higher than that of the QW. This can be observed in Figures 2.c and 2.d. The supralinear growth for the QW temperature is also apparent, and this leads to increasing differences between peak and average temperature as higher power densities are considered. However, as indicated, these are much less relevant than for the QW laser. Also note that the changes in the interface roughness do not play a relevant role for the DH laser.

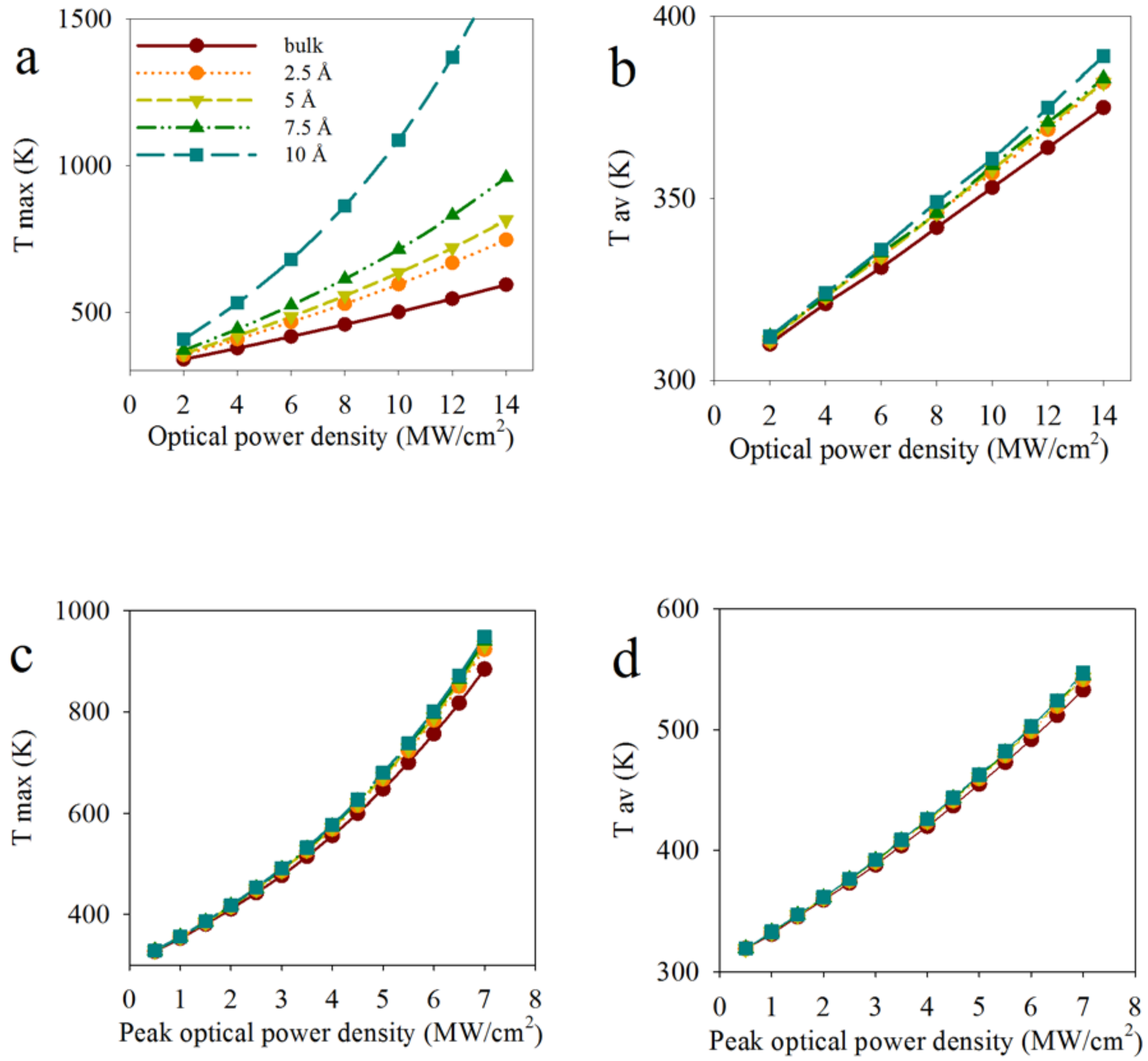

Figure 2. Peak (a) and mean (b) temperatures for the GRINSCH-QW laser as a function of the heat power density source, and for interface roughness ranging from 2.5 to 10 Å. The computed values assuming bulk thermal conductivity are included for comparison purposes. Peak (c) and mean (d) temperatures for the DH laser as a function of the peak heat power density source.

In the frame of our thermo-mechanical model for QW lasers, we initially identified Tc as the temperature at which the thermal stresses induced by the local heating generate dislocations, which occurs when the shear stress reaches the yield strength of the material. This has been discussed in previous articles [7, 9], where it was shown that the computed Tresca (shear) stresses vs local T (peak temperature in the QW) pairs, estimated for different heat power sources and different interface features, were aligned along a straight line, that crosses the experimental curves reported for the yield strength vs T for bulk GaAs at about 480 K. When taking into account the partial suppression of the thermal conductivity, this leads to higher peak temperatures as the interface roughness grows, but the mechanical stresses increase in a correlated manner, so that the Tresca stress - temperature pairs remain all distributed along the same straight line. This is illustrated in Figure 3, where the peak QW T vs Tresca stress computed data are plotted for different values of interface roughness and heat power; the experimental yield strengths for bulk GaAs, as reported in the literature [23, 24], are also depicted. However, our initial estimation was based on peak temperature values, while the experimental Tc reported in the literature correspond to temperatures averaged over the layers surrounding the QW. Assuming QW temperatures of around 500K, the temperature of the adjacent layers is too low to match the experimental data. This suggests the need to reconsider the criterion we followed to define the onset of the mechanical degradation. In fact, we had assumed the starting of the COD to occur when the shear thermal stresses overpass the yield strength of bulk GaAs; however, this approach is probably not fully correct, as one should consider the enhancement of the mechanical strength in nanostructured materials [25-27], which will displace the onset of plasticity of the layers to substantially higher stresses, particularly for the 12 nm QW, while for the DH laser this effect must be significantly less relevant. This point will be treated in forthcoming works.

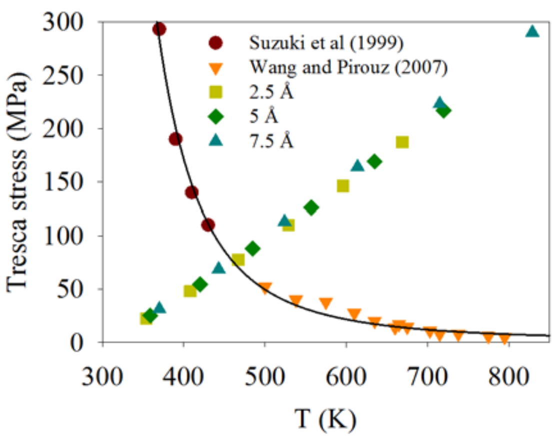

Figure 3. Experimental yield strengths of bulk GaAs, and calculated peak temperature-Tresca stress pairs for different interface roughness values. The computed data where evaluated for power densities ranging from 2 to 12 MW/cm^2 with 2 MW/cm^2 increment steps (yield strength data of bulk GaAs from ref. 23 and 24).

Focusing on the QW laser, more insight into the degradation process can be gathered from Figure 4. This graph represents the computed average temperature versus the QW temperature for various interface roughness values (alternatively, relative amounts of thermal boundary resistance) over an extended power range. The curves for a roughness of 2.5 or 5 Å would correspond to the performance of lasers with the initial QW thermal conductivity [12, 14], if no degradation occurred in the whole temperature range. This is not a realistic assumption, as the elevated peak temperatures reached in the QW would lead to the formation of crystal defects which would lead to increased thermal resistance.

Note that for a given power density, the average temperatures are very similar for the different values of the interface roughness, whereas substantial increments are obtained for the QW temperature due to the increased thermal resistances as the roughness grows. This QW temperature increase will enhance the thermal shear stresses lowering the threshold power for degradation. This mechanism would result in a further decrease of the thermal conductivity, with the concomitant rapid rise of the QW temperature, which could eventually lead to the melting of the QW. Evidence of local melting within the QW has been previously observed for this type of lasers [28].

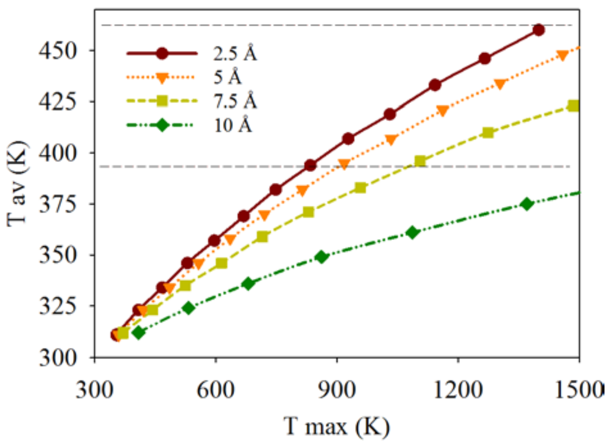

Figure 4. Average vs peak computed temperatures for the GRINSCH-QW laser, for interface roughness ranging from 2.5 to 10 Å. Each individual plot represents the calculated values for power densities ranging from 2 to 26 MW/cm^2 with 2 MW/cm^2 increment steps. The two horizontal lines delimit the experimentally reported Tc values.

The results shown in Figure 4 also reveal a direct connection between the quality of the devices and the (average) critical operation temperature. If, for a given maximum temperature within the QW, one considers the mean value that would be measured on the laser facet, it is clear that the better the thermal conductivity the higher the average temperature estimated for the device. As a matter of fact, if one plots the temperature profiles for similar peak temperatures but for different interface roughness, higher temperature is reached in the guiding and cladding layers when the roughness decreases, which is equivalent to higher Tc, as expected for a more robust device.

5. Conclusions

The thermal distribution due to a local heat source in the active part of a quantum well laser diode has been shown to be very inhomogeneous. We have also demonstrated that the peak temperature is substantially higher than the temperature averaged over the quantum well, the guides and cladding layers; this average temperature can be assimilated to the experimentally measured temperature. In this scenario, the impossibility to directly relate average temperatures to specific physical degradation processes has been addressed, as the physical mechanism driving the degradation seems to be related to the peak temperature in the quantum well, which is significantly higher than the experimentally measured critical temperature.

Acknowledgements

This work was funded by the Spanish Government (Grant: MAT2010-20441-C02-01-02) and Junta de Castilla y León (VA293U13).

REFERENCES

[1] Bettiati M 2013 *Microelectron. Reliab.* **53** 1496

[2] Hempel M, Tomm J W, Hortelano V, Michel N, Jiménez J, Krakowski M and Elsaesser T 2012 *Laser Photon. Rev.* **6** L15

[3] Tang W C, Rosen H J, Vettiger P and Webb D J 1991 *Appl. Phys. Lett.* **58** 557

[4] Ochalski T J, Pierścińska D, Pierściński K, Bugajski M, Tomm J W, Grunske T and Kozlowska A 2006 *Appl. Phys. Lett.* **89** 071104

[5] Nakwaski W 1990 *J. Appl. Phys.* **67** 1659

[6] Smith W R 2000 *J. Appl. Phys.* **87** 8276

[7] Martín-Martín A, Avella M, Iñiguez M P, Jiménez J, Oudart M and Nagle J 2009 *J. Appl. Phys.* **106** 073105

[8] Menzel U 1998 *Semicond. Sci. Technol.* **13** 265

[9] Martín-Martín A, Avella M, Iñiguez M P, Jiménez J, Oudart M and Nagle J 2008 *Appl. Phys. Lett.* **93** 171106

[10] Martín-Martín A, Iñiguez M P, Jiménez J, Oudart M and Nagle J 2011 *J. Appl. Phys.* **110** 033113

[11] Fujii H, Ueno Y and Endo K 1993 *Appl. Phys. Lett.* **62** 2114

[12] Luckyanova M N, Johnson J A, Maznev A A, Garg J, Jandl A, Bulsara M T, Fitzgerald E A, Nelson, K A and Chen G 2013 *Nano Lett.* **13** 3973

[13] Yu X Y, Chen G, Verma A and Smith J S 1995 *Appl. Phys. Lett.* **67** 3554

[14] Capinski W, Maris H, Ruf T, Cardona M, Ploog K and Katzer D 1999 *Phys. Rev. B* **59** 8105

[15] Yao T 1987 *Appl. Phys. Lett.* **51** 1798

[16] Hopkins P E 2013 *ISRN Mech. Eng.* DOI 10.1155/2013/682586

[17] Cheaito R, Duda J C, Beechem T E, Hattar K, Ihlefeld J F, Medlin D L, Rodriguez M A, Campion M J, Piekos E S and Hopkins P E 2012 *Phys. Rev. Lett.* **109** 195901

[18] Zou J, Kotchetkov D, Balandin A A, Florescu D I and Pollak F H 2002 *J. Appl. Phys.* **92** 2534

[19] Liang L H and Li B 2006 *Phys. Rev. B* **73** 153303

[20] Chen G. and Tien C L 1993 *J. Thermophys. Heat Transf.* **7** 311

[21] Ziambaras E and Hyldgaard P 2006 *J. Appl. Phys.* **99** 054303

[22] Gesikowska E and Nakwaski W 2008 *Opt. Quant. Electron.* **40** 205

[23] Suzuki T, Yasutomi T, Tokuoka T and Yonenaga I 1999 *Philos. Mag. A* **79** 2637

[24] Wang S and Pirouz P 2007 *Acta Mater.* **55** 5500

[25] Gerberich W W, Michler J, Mook W M, Ghisleni R, Östlund F, Stauffer D D and Ballarini R 2009 *J. Mater. Res.* **24** 898

[26] Michler J, Wasmer K, Meier S, Östlund F and Leifer K 2007 *Appl. Phys. Lett.* **90** 043123

[27] Zhu T and Li J 2010 *Prog. Mater. Sci.* **55** 710

[28] Hortelano V, Anaya J, Souto J, Jiménez J, Perinet J and Laruelle F 2013 *Microelectron. Reliab.* **53** 1501